



Eco-friendly production of cellulosic fibers from Scots pine wood and sustainable nanosilver modification: A path toward sustainability

K.M. Faridul Hasan^{a,b,*}, Simang Champramary^{c,d}, KM Noman Al Hasan^e, Boris Indic^{c,d}, Taosif Ahmed^{a,b}, Md Nahid Pervez^j, Péter György Horváth^b, Miklós Bak^b, Borza Sándor^b, Tamás Hofmann^f, Laszlo Tolvaj^g, Adrienn Horváth^h, Zsófia Kóczánⁱ, György Sipos^{c,d}, Tibor Alpár^{a,b,**}, László Bejó^{b,***}

^a Fiber and Nanotechnology Program, University of Sopron, Sopron, 9400, Hungary

^b Faculty of Wood Engineering and Creative Industry, University of Sopron, Sopron, 9400, Hungary

^c Department of Microbiology, Faculty of Science and Informatics, University of Szeged, Szeged, Hungary, 9400, Hungary

^d Functional Genomics and Bioinformatics Group, Research Center for Forestry and Wood Industry, University of Sopron, Sopron, 9400, Hungary

^e Department of Textile Engineering, Uttara University, Dhaka, 1230, Bangladesh

^f Institute of Chemistry, Faculty of Forestry, University of Sopron, Sopron, 9400, Hungary

^g Institute of Wood Technology and Technical Sciences, University of Sopron, Sopron, 9400, Hungary

^h Institute of Environmental and Earth Sciences, Faculty of Forestry, University of Sopron, Sopron, 9400, Hungary

ⁱ Paper Research Institute, University of Sopron, Sopron, 9400, Hungary

^j Sanitary Environmental Engineering Division (SEED), Department of Civil Engineering, University of Salerno, via Giovanni Paolo II 132, 84084, Fisciano, SA, Italy

ARTICLE INFO

Keywords:

Defibrination
Scots pine fiber
Green silver nanoparticle
Sustainable coloration
Thermal stability

ABSTRACT

This study presents a novel approach for the production of cellulosic fibers from scots pine wood and their subsequent surface modification with greenly synthesized silver nanoparticles (AgNPs), leading to remarkable color effects and improved functionalities, particularly enhanced thermal stability. The size distribution of the scots pine fiber (SPF) materials was determined through sieve analysis, revealing a conversion of scots pine particles from 1.25 mm to 0.8 mm in size. The AgNPs were biosynthesized in situ on the wood fibers using the same fiber as a sustainable stabilizing and reducing agent. Scanning electron microscopy (SEM) was employed to investigate the morphologies of the control and AgNP-deposited samples, indicating a uniform distribution of nanosilver on the coated surfaces of the SPF material. The concentration of synthesized AgNPs on SPF was quantitatively measured using X-ray fluorescence (XRF) tests, ranging from 4149 ± 43 to 6329 ± 55 parts per million (PPM) depending on the AgNP concentration. The weight percentage of nanoparticles was determined by SEM-mediated energy-disruptive X-ray (EDX) analysis. Additional analyses, Fourier transform infrared spectroscopy (FTIR) test was also conducted. Thermal stability tests demonstrated an improving trend correlated with increasing nanosilver loading in the modified SPF materials. The coefficients of variation (R^2) exhibited a significant relationship between nanosilver loading and most color parameters. Overall, this research presents a pioneering approach for the eco-friendly production of cellulosic fibers from scots pine wood and sustainable synthesis of AgNPs onto defibrated fibers, thus establishing a new benchmark for sustainable manufacturing processes.

Abbreviations: SPF, Scots pine Fiber; AgNPs, Silver nanoparticles; SEM, Scanning electron microscopy; XRF, X-ray fluorescence; PPM, Parts per million; EDX, Energy-disruptive X-ray; FTIR, Fourier transform infrared spectroscopy; R^2 , Coefficients of variation; NPs, Nanoparticles.

* Corresponding author. Fiber and Nanotechnology Program, University of Sopron, Sopron, 9400, Hungary.

** Corresponding author. Fiber and Nanotechnology Program, University of Sopron, Sopron, 9400, Hungary.

*** Corresponding author.

E-mail addresses: faridulwtu@outlook.com, hasan.kmfaridul@uni-sopron.hu (K.M.F. Hasan), alpar.tibor@uni-sopron.hu (T. Alpár), bejo.laszlo@uni-sopron.hu (L. Bejó).

<https://doi.org/10.1016/j.rineng.2023.101244>

Received 3 May 2023; Received in revised form 6 June 2023; Accepted 17 June 2023

Available online 19 June 2023

2590-1230/© 2023 The Authors. Published by Elsevier B.V. This is an open access article under the CC BY-NC-ND license (<http://creativecommons.org/licenses/by-nc-nd/4.0/>).

1. Introduction

Nanotechnology is a rapidly growing interdisciplinary field that will revolutionize the industry as science advances. Materials chemical and physical properties are greatly influenced by their nanostructure features between 1 and 100 nm in size. Nanoparticles' shape, size, surface characteristics, and internal structure are their most distinguishing characteristics. Due to their high surface-to-volume ratio, nanoparticles (NPs) display much higher reactivity, leading to outstanding properties [1–4]. Sometimes, the NPs also influence the electrochemical, thermal, and structural characteristics [5,6] of the products. In some research studies, it has been mentioned that NPs can be employed not only for functionalizing cellulosic materials but also for treating wastewater [7–9]. Recently, the green synthesis of metallic NPs and the functionalization of fibers with sustainable nanocoating have attracted significant customer attention. Different strategies have been developed for multi-NP coating on various synthetic and bio-based cellulose fibers [10]. In particular, NPs are unleashing the fiber, structure, and textile sectors, and through their continuous development, they are bringing significant benefits. However, the characteristic properties of multiple NPs, such as silver, gold, copper, silica, TiO₂, ZnO, and others, are still under explorative investigation. Nevertheless, due to their extraordinary advantages, AgNPs are receiving special attention from scientists nowadays [11]. Not all AgNPs are beneficial for the development of products, as certain chemically synthesized silver nanoparticles can be potentially harmful [12]. Chemical synthesis protocols that were previously widely used by the scientific community are now recognized as not always being safe [13,14]. Therefore, green synthesis protocols are currently gaining popularity. Green silver, created using eco-friendly synthesis processes, is a viable candidate for sustainable applications in fields like fiber functionalization, coatings and medicinal devices because of its many advantages. Research on AgNP synthesis considers different parts of plants as sustainable stabilizers and reducing agents, such as heartwood, stems, leaves, fruits, barks, mushrooms, fungi, and so on [15,16]. However, cellulosic materials such as wood fibers can be used directly as stabilizers and reducing agents. While previous studies have explored natural fibers, there is a lack of research on defibrated cellulose fibers derived from scots pine wood for the purpose of green synthesis of metallic silver in the same bath. This innovative approach has the potential to significantly reduce the usage of chemicals, auxiliaries, and dyes typically employed in the traditional paint industry.

The living plants in our immediate environment provide almost unlimited access to the resources for natural renewable cellulose-containing materials. Among the most popular woody plants, scots pine, poplar, beech, Turkey oak, and hornbeams are the most common in Central European countries, including Hungary [17]. Therefore, scots pine, a widespread species in the European region and one of the vital tree components of the regional economy was selected for this current research on wood fiber and their extracts as the stabilizing agent. We concentrated on defibrating scots pine wood particles to extract the novel cellulosic fibers and then functionalizing them in the same bath with in situ synthesized sustainable AgNPs. Scots pine, like other woods, includes cellulose, hemicellulose, and lignin. It is appropriate for use in the area of the sustainable composite due to its high compatibility with various polymers and chemicals [18]. Moreover, it may have been used to manufacture textile fibers as well. Previously, our research group was interested in developing various structural composites from lignocellulosic particle or fiber reinforced composites [18,19]. We have performed research on cementitious materials reinforced with scots pine for structural applications. Unfortunately, we were unable to use scots pine fiber for composite construction with polymers or cements due to the lack of supporting evidence to be used as the fiber. Consequently, the primary purpose of this study was to defibrate and nanosilver-functionalize pine softwood fibers. This research has the potential to benefit composite manufacturing industries, such as textile and footwear production, as they explore the use of composites that

incorporate novel cellulosic fibers with advanced functionalities. Additionally, sustainable biocomposite and packaging manufacturers could also utilize these SPF fibers. Furthermore, the unique characteristics of these fibers offer diverse opportunities for applications in functional textiles, advanced materials, and environmentally friendly packaging. If SPF could be commercialized for this purpose, the dependence on other cellulosic materials such as fibers, including cotton, flax, hemp, ramie, jute, and others [20–23] could be reduced to the minimum.

Nanotechnology and nanocoated functionalized fibers also show vast economic potential. Therefore, this research aims to defibrate the cellulosic fibers from scots pine wood and use them as stabilizing and reducing agents to produce green metallic silver. They could be used as raw materials for textiles and structural materials like plastic composite products. To date, no results have been reported for defibrated wood-based fiber production from scots pine and to functionalize them with green AgNPs in the same bath. As a result, this is the first report on the feasibility of producing fiber from wood and synthesizing metallic silver over defibrated fibers, with the same fibers also acting as a green stabilizing agent. Furthermore, the various characterizations carried out during this research indicate successful fiber production and AgNP synthesis. Industries may greatly benefit from the current research and novel findings.

2. Materials and methods

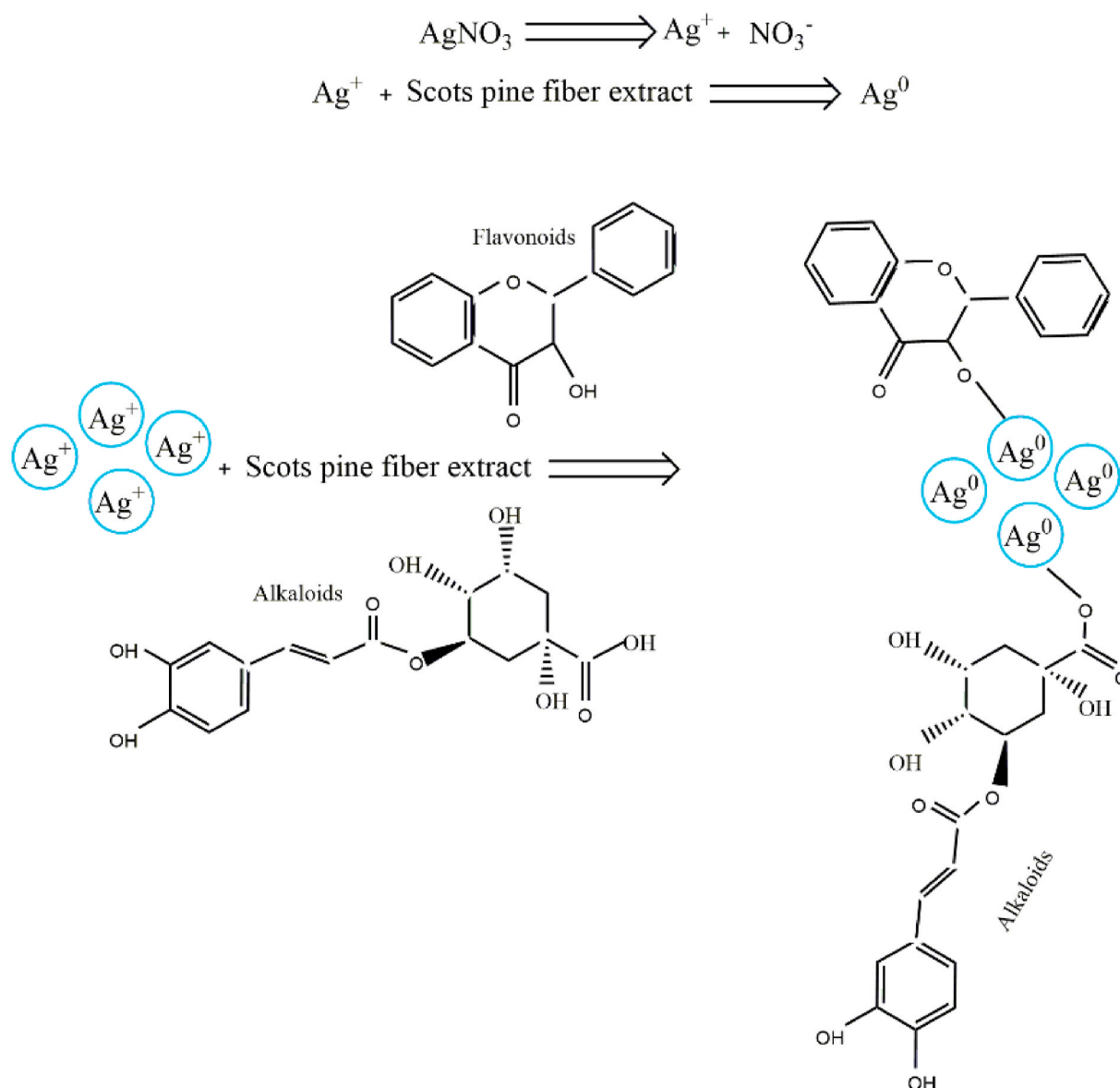
2.1. Materials

Scots pine (*Pinus sylvestris*) wood particles were collected from the Kronospan-MOFA Hungary Ltd. in Mohacs, Hungary. At first, the particles were boiled to produce defibrated cellulosic fibers, then dried at room temperature (25 °C) in a laboratory dryer. AgNO₃ (>90% purity) was purchased from Sigma Aldrich Co., Ltd., United States.

2.2. Methods

2.2.1. Defibration of Scots pine fibers from the wood particles

The scots pine wood particles were defibrated by applying hydrothermal and mechanical processes. The procedure used in this study for the defibration of scots pine fibers from wood particles was reported elsewhere by Maloney [24] with little modifications. Generally, the specific surface of the wood materials is also enlarged by defibrating. In addition, chemically activated compounds in the fibers are also set free, which makes them easier to use for any additional chemical treatments or composite fabrications. There are two main steps to defibrate the fibers from wood: one is to produce chips, and the other is to manufacture fibers from the chips. As a local wood manufacturing company that provided the chips, we made the fibers directly from the pine chips. Another critical aspect of the defibration protocol is plasticizing through steaming, whereby the lignin polymers get softened, the fibers swell, and the chemical structure becomes partially transformed. Wood particles were washed with distilled water and preheated at boiling temperatures (90–100 °C) for 30 min to soften the particles. This also helps form a plug when feeding the chips into a conical screw feeder for continuous compression of the chips in the steaming tube. The plug screw also helps squeeze out some free water in the raw material and/or generated during the operations. This volume varies depending on the type of raw material and line capacity. The defibration process converted the pine chips into fine fiber bundles through the refiner. The refiner was constructed with two discs, one stationary and the other rotating. The scots pine particles were fed into the gap between the hollow stationary disc (middle) and the rotating discs, with a gap distance of about 1 mm. The disc surface contains some raised bars (from coarser to finer). The scots pine particles were propelled by centrifugal forces towards the circumference of the two discs, which gradually helped break them down into their constituent fibers and fiber bundles. The wood species and particle or chip sizes determine the pattern design.



Scheme 1. Proposed schematic representation of silver salt stabilization via scots fibers aqueous solutions.

The gap between the two discs is adjustable, and performing this task requires a lot of water. A discharge port, controlled by a blow-off valve, allows the fibers to exit into the refiner housing. This device adjusted the rate of steam flow and the fiber quantities entering the blow line. The constant production of fibers continued until the parameters were well set and satisfactory quality fibers were generated. Then, finally, the fibers were filtered from the water and squeezed out, followed by drying in laboratory conditions for three days to get dry fibers.

2.2.2. *In situ* biosynthesis of AgNPs

The defibrated SPF's functioned as reducing and stabilizing agents in the aqueous solutions of silver precursor. The fibers were treated with AgNO_3 in the same bath (*in situ*). Therefore, no additional plant extract or chemical-based capping agent was used for this research. However, the aqueous solutions colour began to change at elevated temperatures after a certain time, from the almost colorless milky state to a slightly yellowish, then brownish color. Due to photocatalytic activities, the Ag^+ is reduced to Ag^0 (Scheme 1). These visual and chemical observations confirm the successful formation of metallic silver, and the observed phenomenon also agrees with other studies [25,26]. The defibrated SPF materials (20 g) were placed into a beaker containing 400 mL water

Table 1
Recipe for nanosilver synthesis over SPF material.

Samples	SPF (g)	Silver Precursor (mM)
S@Ag0	–	–
S@Ag1	20	0.5
S@Ag2	20	1.0
S@Ag3	20	1.5

*SPF: Scots pine fiber. mM: Molar weight.

where the M:L (material:liquor) ratio was 1:20. The reason behind the M:L ratio is that the fibers are comparatively bulky. Therefore, they needed more water for better immersion. Later, the AgNO_3 was added to the beakers as per the recipe shown in Table 1. The detailed discussions for sustainable nanosilver synthesis and coating is discussed in our previous articles [27,28]. The development of AgNP should remain on the surface of the SPF's and on the inside of the fibers, which is a challenging task [29]. However, the steaming/cooking process applied as a part of the defibration protocol may render the fibers more accessible for a successful attachment of silver both on the surface and the inside of the SPF. Finally, the beakers were heated at 90 °C for 30 min to ensure a

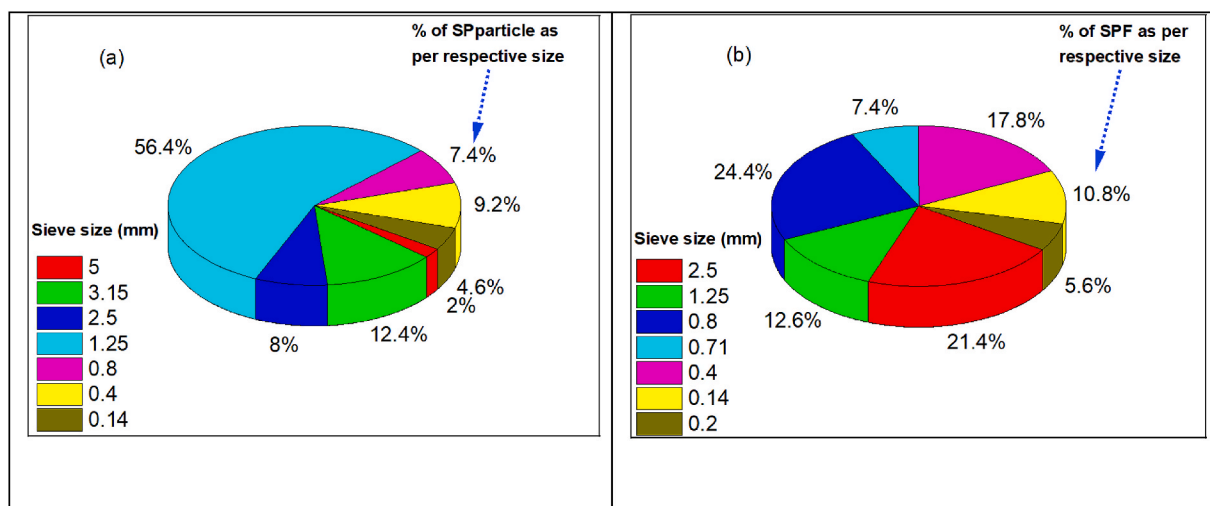


Fig. 1. Size distribution of scots pine particles and fibers.

successful and durable attachment of the AgNPs over the SPF materials. The samples and the beakers were then cooled at the ambient temperature and washed with distilled water. In the end, all the coated SPF materials were dried in the laboratory dryer for 15 min at a high temperature (90 °C) before the characterization.

2.2.3. Characterization of control and AgNP coated SPF fibers

The size distribution of the defibrated fibers was determined through sieve analysis using an ANALYSITTE 3PRO sieve analyzer from Germany. The measurement of deposited AgNPs on the SPF materials was conducted using an XRF testing equipment, specifically the Niton TM XL2 model from ThermoScientific, USA. The readings of the deposited metallic silver were recorded in PPM units after the scanning process. The surface morphologies of the control and AgNP-coated SPF materials were analyzed using a SEM equipment (Hitachi S 3400, Tokyo, Japan) operating at 10.0 kV. The same equipment was also utilized for EDX analysis. For the EDX study, a specialized software called Quantax Esprit 1.9 (Berlin, Germany) was employed. Color characteristics were investigated using a spectrophotometer (Konica Minolta, CM 2600d, Japan) in the 400–700 nm wavelength range, under D65 light. Thermal properties were investigated by a thermal analyzer (Themys thermal analyzer, Setaram Instrumentation, France) under an N₂ atmosphere within a 25–800 °C temperature range. Furthermore, an FTIR test was performed using a spectrophotometer (FT/IR-6300, Jasco, Tokyo, Japan) to analyze the presence of various organic and inorganic chemical molecules within their polymeric structures. The test covered a range of wavelengths from 400 to 4000 cm⁻¹.

3. Results and discussion

3.1. Sieve analysis of scots pine particles and fibers

The control Scots pine samples were sieved before and after the defibration protocols to understand the sizes of the particles and the fibers. Before the defibration, the size range of the particles was between 0.14 and 5.0 mm, whereas the fibers were within 0.2–2.5 mm (Fig. 1). Particles may have been converted into smaller fiber sizes maybe due to the impact of defibration. Most of the particles (56.4%) were within the 1.25–2.5 mm range before defibration, and the second largest fraction was the one below 3.15 mm. After defibration the largest group (24.4%) was 0.8–1.25 mm, followed by fibers larger than 2.5 mm and those between 0.4 and 0.71 mm in size, at 21.4% and 17.8%, respectively. Most particles were smaller than 3.15 mm before fabrication but turned into smaller fractions after conversion into fibers, ranging from 0.4 to

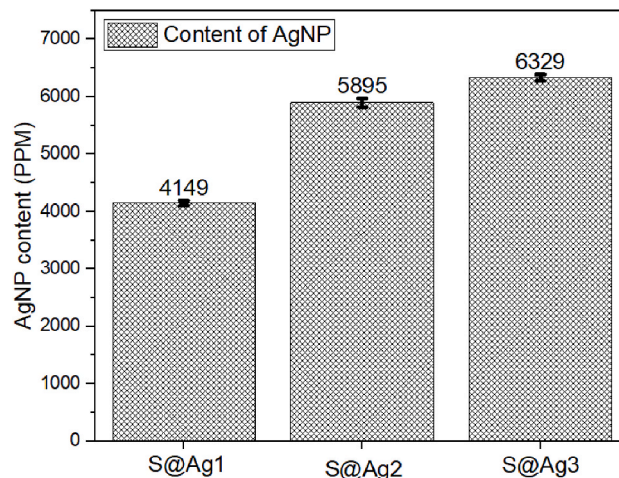


Fig. 2. XRF analysis of AgNP deposited SPF materials.

2.5 mm (most groups amounting to 10–24% in proportion).

3.2. Chemical composition analysis of scots pine fibers

The chemical compounds present in the scots pine were also investigated right after the defibration, where the sizes were maintained in a 0.2–0.6 mm range through sieving to carry out this test. It was found that the fibers contain $59.08 \pm 2.29\%$ holocellulose, $32.32 \pm 1.43\%$ lignin and some other insoluble materials present in the fiber, $0.31 \pm 0.12\%$ ash, and $8.29 \pm 3.72\%$ extractives. The wood of scots pine is categorized as a softwood [30], and in general, all softwood materials contain 56–58% holocellulose and lignin 25–34% [31], therefore, our current findings are in good agreement with the published data.

3.2. Quantification of the deposited AgNPs over the SPF material

The developed AgNPs were quantified through XRF analysis. This is a highly effective method for monitoring the concentrations of NPs over solid surfaces. As expected, the control SPF did not show any presence of nanosilver, as opposed to the other nanoparticle-treated fibers. The highest concentration of AgNPs was displayed by the S@Ag3 sample (6329 ± 55 PPM), where 1.5 mM silver precursors were used. The anticipated lowest proportions of AgNPs were shown by the 0.5 mM precursor treated test specimens at 4149 ± 43 PPM, with the S@Ag2

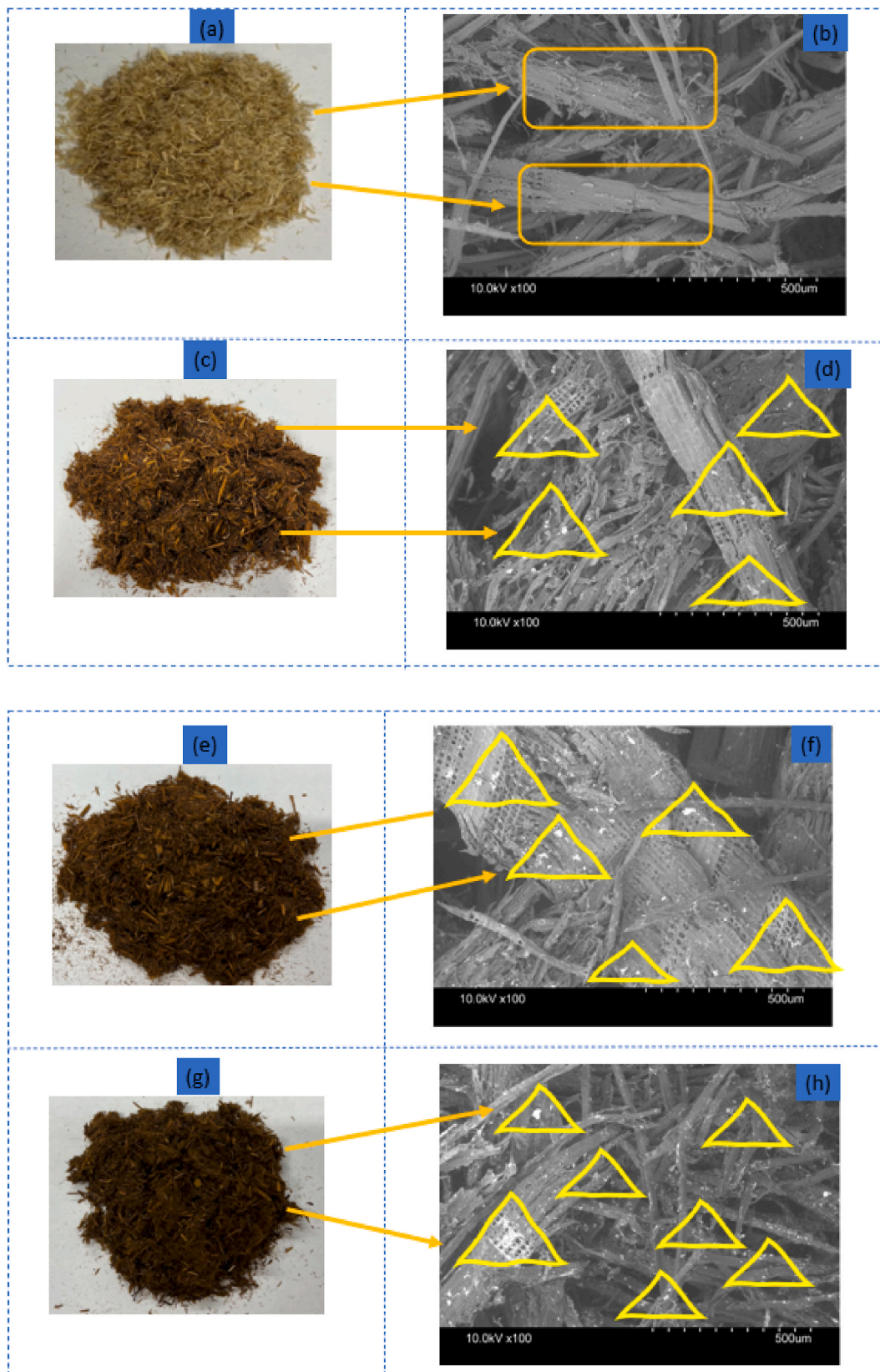


Fig. 3. SEM analysis of control (a and b) and AgNP-deposited SPF materials (details c/d, e/f and g/h corresponding to 0.5, 1.0 and 1.5 mM concentration, respectively).

Table 2

EDX analysis of control and AgNP deposited SPF materials.

Chemical elements	S@Ag0	S@Ag1	S@Ag2	S@Ag3
Carbon	54.58	46.29	41.43	40.53
Oxygen	45.42	40.56	36.65	36.28
Silver	–	13.16	20.77	22.5
Others	–	–	<2.0	<1.0

sample falling in the middle by 5895 ± 75 PPM (1.0 mM AgNO_3 loaded). The concentrations of AgNPs in 1.5 mM and 1.0 mM AgNO_3 treated samples were nearly 53% and 42% higher, respectively than in 0.5 mM precursor treatment (Fig. 2). Increased loading of silver precursors resulted in higher concentrations of AgNPs than control SPF materials, as expected. Similar results were also found in other earlier studies [27, 32].

3.4. Morphological studies of control and AgNP deposited SPF materials

The assembly and development of AgNPs were also investigated further using SEM studies, where control samples did not display any metallic particles, but the treated samples showed homogeneously distributed AgNPs over the SPF surfaces (Fig. 3). The pristine SPF materials had a longitudinal and smooth surface structure. A uniform layer

of nanosized AgNPs was deposited on the surfaces of SPF, demonstrating that the structure of the fibers was not damaged during the functionalization operations [33]. The properties of metallic silver, on the other hand, influence properties such as thermal stability and fiber coloration. The reason behind the deposition of nanoparticles might be that the preheating/cooking of the fibers before defibration facilitated anchoring a better surface for the possible formation of the metallic silver. The developed process may reduce the pressure on traditional natural fibers like cotton and the associated bleaching/scouring operations, that require a lot of dyestuff and chemicals [34]. The nanoparticles are attached not only to the surfaces but also inside the fibres [29]. The isolated NPs of spherical shapes are homogeneously distributed over the SPF surfaces. Like those in the XRF study, SEM images show that higher AgNO_3 loading results in more AgNPs on SPF surfaces.

In addition to the morphological studies, the quantitative values from the EDX study show similar trends to those observed through XRF and SEM analysis. As expected, pristine SPF showed 54.58% C and 45.42% O. However, the proportions of C and O started to decrease with the increased loading of nanosilver. Therefore, SPF samples 1, 2, and 3 contain lower ratios of C and O than the control one. The percentages of AgNPs measured by EDX for 4149, 5895, and 6329 PPM-loaded metallic NPs are 13.16, 20.77, and 22.5%, respectively (Table 2). The distinct peaks of AgNPs are seen at 2.96 keV for the treated samples (Fig. 4). Interestingly, a similar pattern is also seen in the XRF analysis for

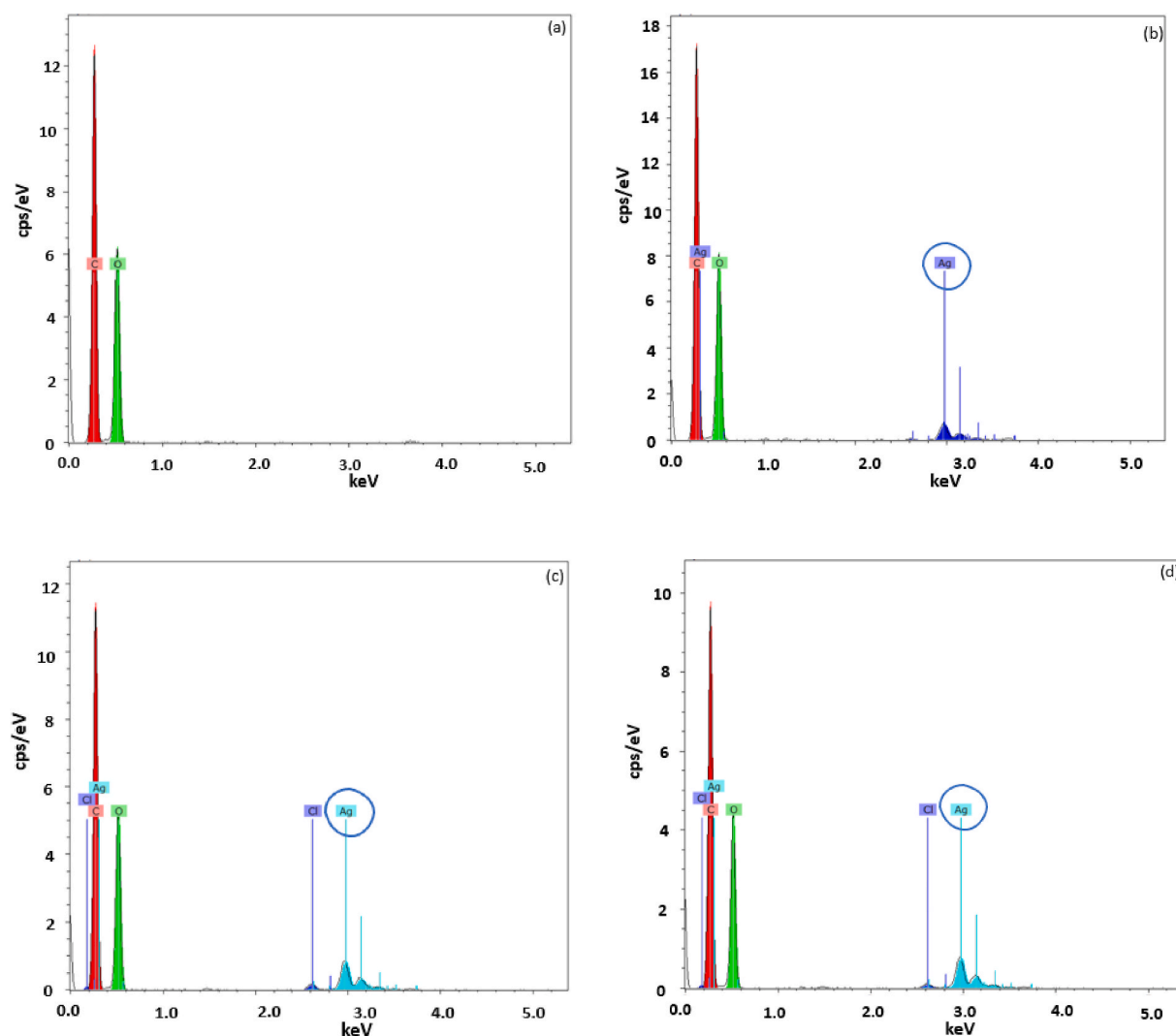


Fig. 4. EDX analysis of control (a) and AgNP-deposited SPF materials (at 0.5, 1.0, and 1.5 mM concentrations, shown in diagrams b, c and d, respectively).

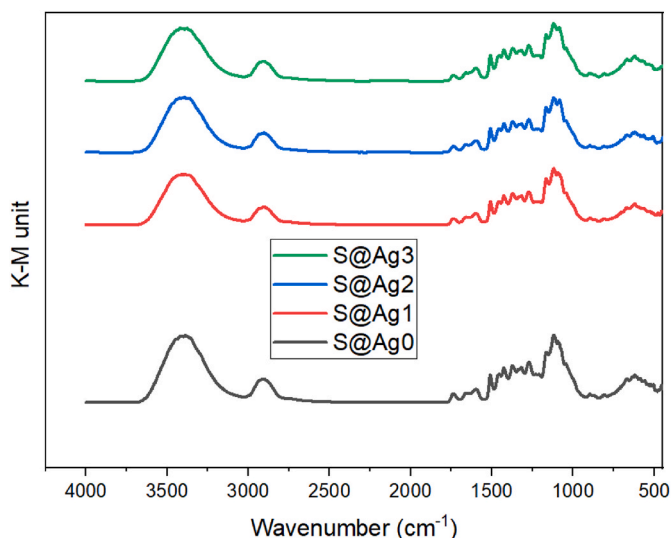


Fig. 5. FTIR analysis of control and AgNP deposited SPF materials.

metallic silver. The results shown here also agree with the previous studies for different naturally stabilized and synthesized metallic silver [15,35]. Overall, the morphological study and EDX analysis discussions confirm the successful formation of metallic silvers over the SPF surfaces.

3.5. FTIR studies of control and AgNP-deposited SPF materials

Fig. 5 shows the IR spectrum of control and AgNP-deposited SPF materials generated by the K-M transformations. The spectra have displayed in the same diagram to understand the comparative differences between the AgNP-coated SPF and control samples. As the control and AgNP-treated materials are fibers obtained from naturally derived woods, they contain cellulose, hemicellulose, and lignin polymers, which is also noticed through the overlapping IR absorbance spectra. Two broad bands are on the left side of the spectra, demonstrating the presence of hydroxyl groups (3400 cm^{-1}). Wood generally absorbs water due to the presence of such hydroxyl groups. The peak at 2900 cm^{-1} is associated with the absorption of prominent C-H stretching. The other peaks at 1735 cm^{-1} are responsible for unconjugated xylans (hemicellulose). Further peaks around 1740 cm^{-1} are responsible for unconjugated carbonyl groups and at 1650 cm^{-1} for conjugated C=O. The presence of aromatic skeletal at lignin is noticed at around 1460

cm^{-1} . Peaks around 1375 cm^{-1} ascribe the deformations of cellulose and hemicellulose polymers in SPF materials. In addition, peaks around 1157 cm^{-1} also show the C-O-C vibrations of SPFs cellulose and hemicellulose polymers. The peaks at 900 cm^{-1} are responsible for the presence of methyl groups. The bands displayed within 900 and 1800 cm^{-1} are the fingerprint of woody materials, which varies from species to species. Typically, the AgNPs are distributed in the cellulosic fibers in the metallic form and produce different metal oxide and metal-OH bonds as the metalorganic compound generally around 1398 to 1125 cm^{-1} wavenumbers which are also in this current study [36,37]. The discussions above also agree with other studies of scots pine and other woods/natural fibers' FTIR analysis [38–40].

3.6. TGA/DTG investigation of control and AgNP-deposited SPF materials

The thermal behaviour of naive and AgNP-deposited fibers was investigated to examine their thermal stability using primary and derivative thermograms of SPF materials (both modified and unmodified with AgNPs). In the case of the naive SPF material, an initial weight loss is observed close to $100\text{ }^\circ\text{C}$ (Fig. 6). The reason behind the initial degradation of weight may be due to the evaporation of moisture from the surface and internal areas of the SPF [41]. The specific weight loss contributions from cellulose, hemicellulose, and lignin may vary depending on the composition and characteristics of the cellulosic fibers, as well as the modification process with nanosilver. The naive SPF showed significant resistance against thermal degradation below $289\text{ }^\circ\text{C}$, and the major decomposition occurs at $405\text{ }^\circ\text{C}$ (accumulating nearly 66% weight loss). The second setep degradation around $289\text{ }^\circ\text{C}$ is related with the hemicellulose decomposition [42]. The degradation around $370\text{ }^\circ\text{C}$ happened due to the presence of cellulose in SPF fibers [42]. Finally, approximately 76% weight loss is observed at $698\text{ }^\circ\text{C}$. However, the differences between the naive and nanosilver-treated samples are slightly different. Interestingly, the increased loading of silver precursors shows slightly higher stability against heat in the case of one-pot green synthesis of AgNPs. Therefore, sample 3 (S@Ag3) showed the highest stability, with 6329 PPM of AgNPs, compared to that of S@Ag2 (5895 PPM) and S@Ag1 (4149 PPM). The increased loading of the metallic silver enhances the collision between the SPF material and the nanoparticles. The maximum degradation is observed at around $700\text{ }^\circ\text{C}$, possibly due to the dehydration of the SPF materials' internal areas. Interestingly, a similar degradation pattern is noticed for the control and AgNP-deposited samples, except for an improvement in thermal stability after nanocoating. The above phenomenon is imperative for using greenly synthesized metallic silver over SPF. Other reports also

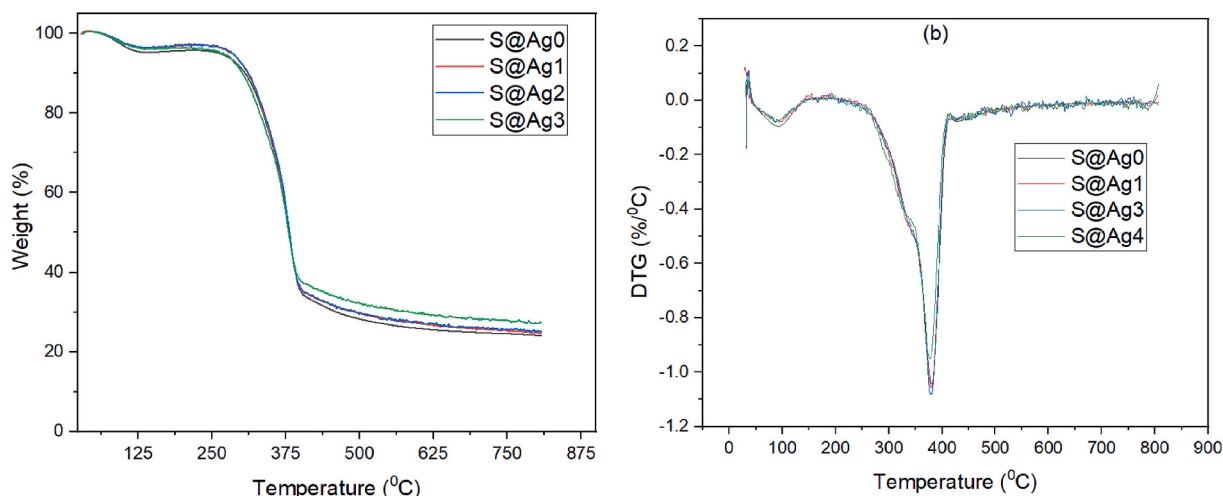


Fig. 6. TGA/DTG analysis of control and AgNP deposited SPF materials.

Table 3
Coloration characteristics of AgNP deposited SPF fibers.

Test specimens	Color strength (K/S)	L*	a*	b*	Assessed color expressions in the coordinates
S@Ag0	0.22	68.65	5.8	27.3	Natural grey color
S@Ag1	6.75	15.16	23.48	25.95	Lighter orange
S@Ag2	8.92	10.38	25.36	17.73	Orange/reddish
S@Ag3	17.13	3.85	18.61	6.47	Dark orange/reddish
R ² (Coefficient of determination)	0.97	0.75	0.4	0.88	

documented similar effects for diversified greenly synthesized AgNPs [43,44].

3.7. Color characteristics of the SPF material

Brilliant and remarkable colorful effects are seen on the SPF materials, possibly due to the presence of LSPR (localized surface plasmon resonance) optical characteristics of AgNPs that were introduced over the fibers through adopting an in situ synthesis protocol without applying any conventional dyestuff, chemicals, and or auxiliaries. Fig. 3 shows photographs of pristine and treated SPF materials. The pristine fibers did not show any colorful appearance, only a grey color. However, the treated SPF samples show brilliant coloration effects, which get darker with the increase in nanosilver loading. The color values (L*, a*, b*, and K/S color strength) were measured for control, 0.5, 1.0, and 1.5 mM AgNO₃ loaded samples. The colorful fiber may be used to produce textile yarns, nonwoven mats, and structural composites industrially with improved functionalities. It is noticed that the K/S values show an increasing trend with the increase in AgNP loading. As expected, the control AgNPs had the lowest K/S value of only 0.22, whereas the 1.5 mM silver precursor-loaded samples achieved the highest value (17.13). Compared to the control sample where no AgNO₃ was used, 0.5 mM, 1.0 mM, and 1.5 mM silver precursor-treated samples showed 30, 40, and 78 times higher color strength values, respectively (Table 3). A similar pattern also emerges for L* values, where higher incorporation of metallic silver provides higher L* values. However, a* and b* values do not follow this tendency, with b* being negatively correlated with AgNP loading and a* showing no clear trend. The coefficient of determination was calculated for each color parameter and indicated a significant relationship between increased nanosilver precursor loads and most color properties. Although the R² value for a* is low, it is much higher in the case of K/S (0.97), L* (0.75), and b* (0.88). These results agree well with previous studies [27].

4. Conclusion

This investigation highlights a cost-effective, innovative, and environmentally friendly approach for defibrating fiber manufacturing from Scots pine softwood and synthesizing silver using the same fiber. The extracted fibers are functionalized by sustainable AgNPs synthesized with the same fiber as the stabilizing agent. Higher concentrations of silver precursor led to increased production of AgNPs, as confirmed by XRF, SEM, and EDX studies. Additionally, SPF K/S values also increased with higher silver precursor loading in the synthesis bath. The absence of additional stabilizing or reducing agents in the metallic particle synthesis presents a convenient and feasible method that could inspire the coloration industry with a new idea and product. The production of fibers from wood offers fiber manufacturing companies a novel alternative for structural and construction materials. The FTIR study demonstrates strong interaction between the fibers and metallic silver, indicating the presence of cellulosic molecules in the fiber substrate. Furthermore, the application of nanosilver coating improves the thermal stability of SPF materials, which is further enhanced with increased NP

loading.

CrediT authorship contributor statement

K. M. Faridul Hasan: Conceptualization, Methodology, Investigation, Visualization, Writing – original draft. **Simang Champramary:** Conceptualization, Methodology, Investigation, Visualization, Writing – original draft., **KM Noman Al Hasan:** Methodology, Investigation, Visualization, Writing – original draft., **Boris Indic:** Methodology, Investigation, Visualization, Writing – original draft., **Taosif Ahmed:** Methodology, Investigation, Visualization, Writing – original draft., **Md Nahid Pervez:** Investigation, Visualization, Writing – original draft., **Péter György Horváth:** Resources, Supervision, Writing – review final draft, **Miklós Bak:** Methodology, Investigation, Visualization. **Borza Sándor:** Resources, Supervision, Writing – review final draft., **Tamás Hofmann:** Methodology, Investigation, Visualization, Writing – original draft. **Laszlo Tolvaj:** Methodology, Investigation, Visualization., **Adrienn Horváth:** Methodology, Investigation, Visualization., **Zsófia Kóczán:** Methodology, Investigation, Visualization, **György Sipos:** Conceptualization, Resources, Writing – review final draft., and **Tibor Alpár:** Conceptualization, Resources, Supervision, Writing – review final draft., **László Bejő:** Resources, Supervision, Writing – review final draft.

Funding

This work did not receive any additional funding.

Declaration of competing interest

The authors declare that they have no competing interest for the submitted work.

Data availability

Data will be made available on request.

Acknowledgement

This article was produced within the framework of “TKP2021-NKTA-43” project with the support provided by the Ministry of Innovation and Technology of Hungary from the National Research, Development and Innovation Fund, financed under the TKP2021-NKTA funding scheme. Authors are also grateful to Kun Gábor, (University of Sopron) for his cooperations during this research.

References

- [1] I.S. Tania, M. Ali, Coating of ZnO nanoparticle on cotton fabric to create a functional textile with enhanced mechanical properties, *Polymers* 13 (2021) 2701, <https://doi.org/10.3390/polym13162701>.
- [2] K.F. Hasan, et al., Functional silver nanoparticles synthesis from sustainable point of view: 2000 to 2023–A review on game changing materials, *Heliyon* 8 (2022), e12322, <https://doi.org/10.1016/j.heliyon.2022.e12322>.
- [3] M. Iqbal, et al., Facile synthesis of Cr doped hierarchical ZnO nano-structures for enhanced photovoltaic performance, *Inorg. Chem. Commun.* 116 (2020), 107902.
- [4] J. Khan, et al., High yield synthesis of transition metal fluorides (CoF₂, NiF₂, and NH₄MnF₃) nanoparticles with excellent electrochemical performance, *Inorg. Chem. Commun.* 130 (2021), 108751.
- [5] S. Hussain, et al., Effect of iron oxide co-doping on structural, thermal, and electrochemical properties of samarium doped ceria solid electrolyte, *Mater. Chem. Phys.* 267 (2021), 124576.
- [6] T.C. Egbosiuba, et al., Adsorption of Cr (VI), Ni (II), Fe (II) and Cd (II) ions by KIAGNPs decorated MWCNTs in a batch and fixed bed process, *Sci. Rep.* 11 (2021) 75.
- [7] S. Aliyu, et al., Development of Ag-doped on multi-walled carbon nanotubes for the treatment of fish pond effluent, *Regional Studies in Marine Science* 58 (2023), 102797.
- [8] T.C. Egbosiuba, et al., Activated multi-walled carbon nanotubes decorated with zero valent nickel nanoparticles for arsenic, cadmium and lead adsorption from

- wastewater in a batch and continuous flow modes, *J. Hazard Mater.* 423 (2022), 126993.
- [9] A.S. Kovo, et al., Column adsorption of biological oxygen demand, chemical oxygen demand and total organic carbon from wastewater by magnetite nanoparticles-zeolite A composite, *Heliyon* 9 (2023).
- [10] L. Jiang, et al., Preparation of antimicrobial activated carbon fiber by loading with silver nanoparticles, *Colloids Surf. A Physicochem. Eng. Asp.* 633 (2022), 127868, <https://doi.org/10.1016/j.colsurfa.2021.127868>.
- [11] S. Mishra, H. Singh, Biosynthesized silver nanoparticles as a nanoweapon against *Staphylococcus aureus* exploring their scope and potential in agriculture, *Appl. Microbiol. Biotechnol.* 99 (2015) 1097–1107.
- [12] K. Chand, et al., Green synthesis characterization and antimicrobial activity against *Staphylococcus aureus* of silver nanoparticles using extracts of neem, onion and tomato, *RSC Adv.* 9 (2019) 17002–17015.
- [13] S. Marimuthu, et al., Silver nanoparticles in dye effluent treatment: a review on synthesis, treatment methods, mechanisms, photocatalytic degradation, toxic effects and mitigation of toxicity, *J. Photochem. Photobiol. B Biol.* 205 (2020), 111823, <https://doi.org/10.1016/j.jphotobiol.2020.111823>.
- [14] M.N. Pervez, et al., Nanomaterial-based smart and sustainable protective textiles, in: *Protective Textiles from Natural Resources*, Woodhead Publishing, 2022, pp. 75–111.
- [15] K.F. Hasan, et al., Green synthesis of nanosilver using *Fomes fomentarius* mushroom extract over aramid fabrics with improved coloration effects, *Textil. Res. J.* (2022), 00405175221086892, <https://doi.org/10.1177/00405175221086892>.
- [16] S. Irvani, B. Zolfaghari, Green synthesis of silver nanoparticles using *Pinus eldarica* bark extract, *BioMed Res. Int.* 2013 (2013), 639725, <https://doi.org/10.1155/2013/639725>.
- [17] K.F. Hasan, P.t.G.r. Horváth, T. Alpár, *Nanotechnology for waste wood recycling*, in: *Nanotechnology in Paper and Wood Engineering*, Woodhead Publishing, Duxford, United Kingdom, 2022, pp. 61–80.
- [18] K.F. Hasan, et al., Semi-dry technology-mediated coir fiber and Scots pine particle-reinforced sustainable cementitious composite panels, *Construct. Build. Mater.* 305 (2021), 124816, <https://doi.org/10.1016/j.conbuildmat.2021.124816>.
- [19] K.F. Hasan, P.G. Horváth, T. Alpár, Development of lignocellulosic fiber reinforced cement composite panels using semi-dry technology, *Cellulose* 28 (2021) 3631–3645, <https://doi.org/10.1007/s10570-021-03755-4>.
- [20] S. Mahmud, et al., Comprehensive review on plant fiber-reinforced polymeric biocomposites, *J. Mater. Sci.* 56 (2021) 7231–7264, <https://doi.org/10.1007/s10853-021-05774-9>.
- [21] Tibor, L.A., G.H. Péter, and K.M.F. Hasan, Introduction to biomass and biocomposites, in *Toward the Value-Added Biocomposites: Technology, Innovation and Opportunity*. 2021, CRC Press: Boca Raton, USA. p. 1-33.
- [22] Z.M. Mucsi, et al., Semi-dry technology mediated lignocellulosic coconut and energy reed straw reinforced cementitious insulation panels, *J. Build. Eng.* 57 (2022), 104825, <https://doi.org/10.1016/j.jobbe.2022.104825>.
- [23] K.F. Hasan, et al., Physicochemical and morphological properties of microcrystalline cellulose and nanocellulose extracted from coir fibres and its composites, in: M. Jawaid (Ed.), *Coir Fiber and its Composites Processing, Properties and Applications*, Woodhead Publishing, Elsevier, Cambridge, United Kingdom, 2022, pp. 255–267.
- [24] T. Maloney, Raw materials and particle geometry: effects on board properties, in: *Modern Particleboard and Dry-Process Fiberboard Manufacturing*, Miller Freeman Inc., San Francisco, California, USA, 1993, pp. 178–212.
- [25] S. Eustis, M.A. El-Sayed, Why gold nanoparticles are more precious than pretty gold: noble metal surface plasmon resonance and its enhancement of the radiative and nonradiative properties of nanocrystals of different shapes, *Chem. Soc. Rev.* 35 (2006) 209–217, <https://doi.org/10.1039/B514191E>.
- [26] A. Lakshmanan, S. Chakraborty, Coating of silver nanoparticles on jute fibre by in situ synthesis, *Cellulose* 24 (2017) 1563–1577, <https://doi.org/10.1007/s10570-017-1204-2>.
- [27] K.F. Hasan, et al., Colorful and facile in situ nanosilver coating on sisal/cotton interwoven fabrics mediated from European larch heartwood, *Sci. Rep.* 11 (2021) 1–13, <https://doi.org/10.1038/s41598-021-01914-y>.
- [28] K.F. Hasan, et al., Nanosilver Coating on Hemp/cotton Blended Woven Fabrics Mediated from Mammoth Pine Bark with Improved Coloration and Mechanical Properties, *J Text Inst*, 2021, pp. 1–10.
- [29] G. Montes-Hernandez, et al., In situ formation of silver nanoparticles (Ag-NPs) onto textile fibers, *ACS Omega* 6 (2021) 1316–1327, <https://doi.org/10.1021/acsomega.0c04814>.
- [30] S. Metsämuuronen, H. Sirén, Bioactive phenolic compounds, metabolism and properties: a review on valuable chemical compounds in Scots pine and Norway spruce, *Phytochemistry Rev.* 18 (2019) 623–664, <https://doi.org/10.1007/s11101-019-09630-2>.
- [31] S.K. Gulsoy, F. Ozturk, Kraft pulping properties of European black pine cone, *Maderas Cienc. Tecnol.* 17 (2015) 875–882, <https://doi.org/10.4067/S0718-221X2015005000076>.
- [32] K.F. Hasan, et al., Coloration of flax woven fabric using *Taxus baccata* heartwood extract mediated nanosilver, *Colour. Technol.* 138 (2021) 146–156, <https://doi.org/10.1111/cote.12578>.
- [33] S. Mahmud, et al., Surface functionalization of “Rajshahi Silk” using green silver nanoparticles, *Fibers* 5 (2017) 35, <https://doi.org/10.3390/fib5030035>.
- [34] M.E. El-Naggar, S. Shaarawy, A. Hebeish, Bactericidal finishing of loomstate, scoured and bleached cotton fibres via sustainable in-situ synthesis of silver nanoparticles, *Int. J. Biol. Macromol.* 106 (2018) 1192–1202, <https://doi.org/10.1016/j.ijbiomac.2017.08.127>.
- [35] K.F. Hasan, et al., Enhancing mechanical and antibacterial performances of organic cotton materials with green synthesized colored silver nanoparticles, *Int. J. Cloth. Sci.* 34 (2022) 549–565, <https://doi.org/10.1108/IJCST-05-2021-0071>.
- [36] O. Rac-Rumijowska, et al., Multifunctional nanocomposite cellulose fibers doped in situ with silver nanoparticles, *Polymers* 11 (2019) 562, <https://doi.org/10.3390/polym11030562>.
- [37] A. Azari, et al., Iron–silver oxide nanoadsorbent synthesized by co-precipitation process for fluoride removal from aqueous solution and its adsorption mechanism, *RSC Adv.* 5 (2015) 87377–87391, <https://doi.org/10.1039/C5RA17595J>.
- [38] K. Pandey, A. Pitman, FTIR studies of the changes in wood chemistry following decay by brown-rot and white-rot fungi, *Int. Biodeterior. Biodegrad.* 52 (2003) 151–160, [https://doi.org/10.1016/S0964-8305\(03\)00052-0](https://doi.org/10.1016/S0964-8305(03)00052-0).
- [39] K.M.F. Hasan, et al., Thermo-mechanical characteristics of flax woven fabric reinforced PLA and PP biocomposites, *Green Mater.* 10 (2021) 1–10, <https://doi.org/10.1680/jgrma.20.00052>.
- [40] E. Preklet, et al., Effect of water leaching on photodegraded Scots pine and spruce timbers monitored by FTIR spectroscopy, *Forests* 12 (2021) 833, <https://doi.org/10.3390/f12070833>.
- [41] C.K. Kang, et al., Antibacterial cotton fibers treated with silver nanoparticles and quaternary ammonium salts, *Carbohydr. Polym.* 151 (2016) 1012–1018, <https://doi.org/10.1016/j.carbpol.2016.06.043>.
- [42] D.P. Ferreira, et al., Smart and sustainable materials for military applications based on natural fibres and silver nanoparticles, in: *Key Engineering Materials, Trans Tech Publ*, 2019.
- [43] S. Mahmud, et al., Multifunctional organic cotton fabric based on silver nanoparticles green synthesized from sodium alginate, *Textil. Res. J.* 90 (2019) 1224–1236, <https://doi.org/10.1177/0040517519887532>.
- [44] B. Ashok, et al., Modification of natural fibers from *Thespesia lampas* plant by in situ generation of silver nanoparticles in single-step hydrothermal method, *Int. J. Polym. Anal. Char.* 23 (2018) 509–516, <https://doi.org/10.1080/1023666X.2018.1486270>.